RSC Advances

PAPER

View Article Online
View Journal | View Issue

Cite this: *RSC Adv.*, 2014, **4**, 1900

Microfluidic preparation and structure evolution of double emulsions with two-phase cores†

Jian-Hong Xu,* Xue-Hui Ge, Ran Chen and Guang-Sheng Luo

Received 18th October 2013
Accepted 20th November 2013

DOI: 10.1039/c3ra46562d

www.rsc.org/advances

In this work, we developed a simple capillary microfluidic device to prepare double emulsions with two-phase cores. We can control the structure and size of double emulsions by changing four-phase flow rates. Based on the formation of these four-phase double emulsions, we investigated the structure evolution of the double emulsions for different systems, and successfully obtained different multiple emulsions with four typical inner structures, as a separately engulfing structure, triple emulsion structure, Janus-engulfing structure, and inner-Janus structure. The equilibrium morphologies of the double emulsions could be estimated by using the relationship of interfacial tension between different phase fluids. Remarkably, the physics of evolution of double emulsions with two-phase cores in a microfluidic device allows the synthesis of microparticles with new morphologies and more applications in encapsulation of multiple active substances.

Introduction

Multiple emulsions have attracted considerable attention because of their high potential for applications in the fields of controlled substance release[1,2] separation,[3] food science,[4] cosmetics,[4] pharmaceuticals,[5] bio-compatibility[6] and the textile industry.[7] However, previous researches using traditional methods, for example, a two-step procedure of emulsification,[8] have many disadvantages such as poly dispersed emulsions, uncontrollability in emulsion size and distribution, and deficiency in regulation of the inner droplets. These disadvantages were resolved in the past decade when microfluidic technology were widely used in the preparation of mono-dispersed emulsions, which has enabled the formation of multiple emulsions with controlled droplet sizes, structures, and compositions.[9]

In addition, multiple emulsions with different components in the inner droplets provide wider application in fields such as drug delivery and the production of multi-compartment materials.[10,11] Researchers using micro-capillary or microchip devices obtained monodispersed multi-component emulsions with good control in the number of droplets at each level.[11] By scaling up three basic units, a drop maker, a connector and a liquid extractor, Chu *et al.*[12] made further progress to prepare higher-order multi-component multiple emulsions with precise control of the number, ratio and size of differentiated droplets in each level. Recently, Adams *et al.*[13] achieved exactly the same accurate control by utilizing a single step emulsification technique which made the production and application of multi-components emulsions more practical than before. However, the above progress focused only on the production of multi-component multiple emulsions. For the fields in which different phases of inner droplets are required, for example, in cosmetics in which water-soluble and oil-soluble active substance are both required to be encapsulated, multi-component multiple emulsions could not meet the demands. Therefore, the development of multiple emulsions with multi-phase cores in the same internal level is highly imperative.

Moreover, the morphologies of multiple emulsions have attracted considerable interests because of their significant potential in application, including functional materials,[14] medicine,[15] ultrasonic imaging,[16] and micro-crawls.[17] Multiple emulsions could be a good template for preparing particles with different structures by polymerizing droplets in a chosen level.[18,19] Researchers have obtained different morphologies with the same liquids and they could draw a phase diagram to describe that.[20] N. Pannacci *et al.*[21] have furthered this work by explaining that the possibility of different structures formed within same liquids is because the emulsions are in different states, *i.e.* equilibrium and non-equilibrium structures. The equilibrium structures are determined by the minimum interfacial energy of three immiscible phases which formed a three-phase system. And there are three possible morphologies depending on the spreading coefficients related to the interfacial tension between every couple phases in a three-phase

The State Key Lab of Chemical Engineering, Department of Chemical Engineering, Tsinghua University, Beijing 100084, China. E-mail: xujianhong@tsinghua.edu.cn; Fax: +86-10-62773017; Tel: +86-10-62773017

† Electronic supplementary information (ESI) available: Fig. S1–S4 (formation rules of double emulsion with single phase core); Movies S1 and S2 (formation process of double emulsion with two-phase core in the droplet forming area); Movies S3–S5 (the structure evolution process of the double emulsions of different systems); and Table S1 (specific interfacial tensions for different systems). See DOI: 10.1039/c3ra46562d

system, for which the mathematic relationship was derived by Torza *et al.*[22]

The three possible equilibrium morphologies are completely engulfing structures, partial engulfing structure (Janus), and non-engulfing structure. Together with the non-equilibrium morphologies formed in the process toward an equilibrium state, microparticles with new morphologies can be formed by solidifying these emulsions. This has provided an essential method to produce novel polymer microparticles with diversified structures. Inspired by this principle, we hypothesized that if we introduce another immiscible phase into the three-phase system, which meant the system would be composed of four immiscible phases, more interesting structures which might be well beyond the possibilities of traditional technologies may be obtained. Herein, we introduce the fourth phase to synthesis double emulsions with two-phase cores, which, to the best of our knowledge, had not been explored before.

In this work, we firstly synthesized double emulsion with two-phase inner cores by using a simple one-step microfluidic approach. Then we investigated the structure evolution process of the double emulsions for different systems and obtained different multiple emulsions with four typical inner structures. Moreover, we measured interfacial tension between each immiscible phase and analyzed the relationship between the equilibrium morphology and the interfacial tensions of these four-phase systems. We found that the equilibrium morphologies of the double emulsions with two-phase cores are also determined by the minimum of interfacial energy of the system. Based on it, the physics of the structure evolution of double emulsions with two-phase cores allows the synthesis of microparticles with new morphologies and more applications in the encapsulation of multiple active substances.

Experimental and methods

Fabrication of the microfluidic device

Two cross junctions are fabricated on a 40 mm × 25 mm × 7 mm polymethyl methacrylate (PMMA) chip using an end mill. The two inner phase fluids are introduced trough the parallel micro-needles with inner-diameter of 160 μm and outer-diameter of 300 μm. The channel for middle and outer phase fluids is approximately 1.50 mm wide × 1.50 mm high, as shown in Fig. 1. A circular glass capillary with 1.05 mm inner-diameter and 1.5 mm outer-diameter is tapered using a micropipette puller (P-97, SUTTER Co. Ltd., USA) for the injection of the middle phase fluid. The diameter of the tapered orifice is approximately 340 μm. The first tapered capillary is inserted into a second capillary for the outer phase and coaxality is guaranteed by matching the outer diameter of the capillary with the inner dimension of the channel. The second capillary is not tapered. Six PTFE pipes are inserted into sides of the chip channel for carrying middle and outer phase fluids. Four micro-syringe pumps (LSP01-1B, Baoding Longer Precision Pump Co. Ltd.) are used to pump the four-phase system into the microfluidic device respectively.

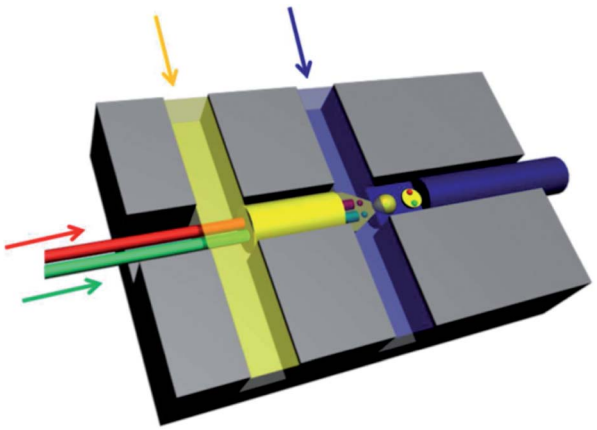

Fig. 1 The parallel co-flowing coaxial microfluidic device used in the experiments. Red and green flows represent two inner-phase flows, they could be either silicon oil, deionized water with surfactant, tetradecane or gas, red flow and green flow contain two insoluble phases. Yellow and blue flows represent middle and outer phase flows. Yellow flow could be either TPGDA, HDDA or silicon oil. Blue flow is deionized water with 2% SDS and 1% PVA. Inner-phase flows are pumped into microfluidic device through two micro-needles, middle phase flow encapsulates them to form a first structure red & green droplets/yellow flow, then outer flow engulfs the structure, so a red & green droplets/yellow droplet double emulsion is formed. To demonstrate the microfluidic device clearly, we make a cross section in the droplet forming area.

Preparation of double emulsions with two-phase cores

We drive four immiscible fluids into the microfluidic device to produce double emulsions with two-phase cores. Two inner-phase flows in the micro-needles are sheared into droplets by middle phase flow. Middle flow in the cylindrical capillary is sheared into droplet within two inner droplets at the tapered end by the outer phase flow. By tuning the flow rates of micro-syringe pumps, the sizes and the number of engulfed inner droplets could be controlled precisely. The working fluids are silicon oil with the viscosity of 50 mPa s and 100 mPa s (Jing Pinghua Co. Ltd), tripropylene glycol diacrylate (TPGDA, J&K CHEMICA Co. Ltd), tetradecane (J&K CHEMICA Co. Ltd), 1,6-hexanediol diacrylate (HDDA, ALDRICH Chemistry Co. Ltd), mineral oil, deionized water with 2.0 wt% sodium dodecyl sulfate (SDS) surfactant and 1.0 wt% polyvinyl alcohol (PVA, average molecular weight: 1750) for increasing fluid viscosity. Dow Corning 749, purchased from Dow Corning Co. Ltd., is used as the emulsifier in the oil phase with the concentration of 10 wt% to stabilize droplets. All the reagents are analytically pure and used as received.

Analysis of the evolution of double emulsions

The evolution of the double emulsions was carried out with an optical microscope (BX61, Olympus, Japan) equipped with a high-speed camera with adjustable frequency (B742, Pixelink, Canada). Typical orders of magnitude of inner, middle and outer flows are 1 μL min^{-1}, 10 μL min^{-1}, and 100 μL min^{-1}, respectively. The typical sizes of inner and middle droplets are 200 μm and 1500 μm. During the experiments, Reynolds and

capillary numbers are small. The surface tension (gas–liquid) and interfacial tension (liquid–liquid) was measured by an interfacial tension meter using the pendent drop technique (OCAH200, DataPhysics Instruments GmbH, Germany). All the experiments were carried out at room temperature.

Results and discussion

Formation of double emulsions with two-phase cores

To test the usability of the microfluidic device, we first drove only one phase into a microneedle while the other one was sealed to produce W/O/W double emulsion. We successfully obtained monodispersed double emulsions with accurate control in the number and the size of the inner droplets (see in ESI Fig. S1–S4†).

On this basis, we injected air gas and aqueous phases into the micro-needles which were encapsulated by the oil phase and then gas & water/oil structure was formed, another aqueous phase was injected as outer phase fluid to engulf the structure, thus double emulsions with gas microbubble and aqueous droplet in the core, as a gas & water/oil/water double emulsion was formed. The formation process of the gas & water/oil/water double emulsion can be seen in the ESI (see Movie S1†). We could control the size and the ratio of inner droplets by adjusting the flow rates of four-phase fluids. As the two inner-phase flow rates increase, the number of the encapsulated droplets and microbubbles per oil plugs increases with the increased frequency of the formed inner droplets and microbubbles. Fig. 2 shows the typical micrographs of gas & water/oil/water double emulsion with increased number and ratio of encapsulated inner droplets and microbubbles.

Then, we used an oil phase to replace gas while the other phases stayed the same. We synthesized double emulsions with oil phase and aqueous phase in the core, as oil & water/oil/water double emulsion. We also adjusted the flow rates of four-phase fluids to control the size and ratio of inner droplets. Fig. 3 shows the typical micrographs of oil & water/oil/water double emulsion with increased number and ratio of oil droplets to aqueous droplets. (Formation process in the droplet forming area can be seen in ESI for Movie S2†.)

Furthermore, the parallel co-axial capillary microfluidic device has the advantage that we can obtain either O/W/O or inverse W/O/W double emulsions in the same geometry without surface modification of wettability. We drove two immiscible oils as the inner phases, another immiscible oil phase as the middle phase, and aqueous phase as outer phase, thus double emulsion with two immiscible oil phases in the core, as oil & oil/oil/water double emulsion was formed, as shown in Fig. 4c. Herein, we have four immiscible phases in this situation, which is basic for the latter research in interfacial tension measurement and analysis to explain the equilibrium morphology of double emulsions with two-phase cores.

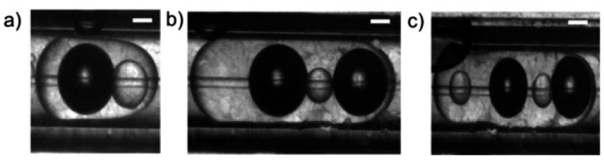

Fig. 2 The typical micrographs of gas & water/oil/water double emulsion with increased number and ratio of encapsulate inner droplets and microbubbles. These were observed in the outer flow channel. The black and big one is microbubble and the other is aqueous droplet. The ratio of number of microbubbles to aqueous droplets is (a) 1 : 1; (b) 2 : 1; (c) 2 : 2. The fluids are water + 1% PVA + 2% SDS & air/silicon oil (50 cp) + 10% Dow corning 749/water + 1% PVA + 2% SDS. The scale bar is 200 μm.

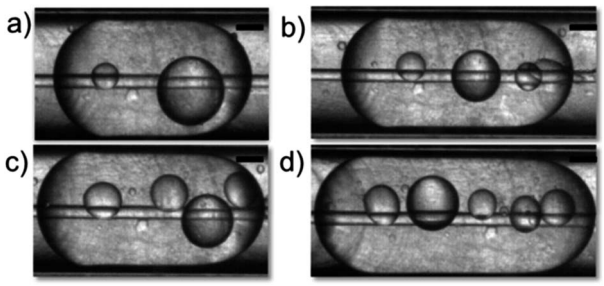

Fig. 3 The typical micrographs of oil & water/oil/water double emulsion with increased number and ratio of encapsulated inner droplets. These were observed in the outer flow channel. The big one is aqueous droplet and the other is oil droplet. The number ratio of oil droplets to aqueous droplets are (a) 1 : 1; (b) 2 : 1; (c) 3 : 1; (d) 4 : 1. The fluids are water + 1% PVA + 2% SDS & TPGDA/silicon oil (50 cp) + 10% Dow corning/water + 1% PVA + 2% SDS. The scale bar is 200 μm.

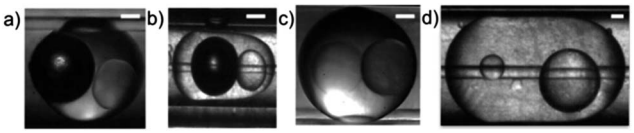

Fig. 4 The typical types of double emulsion with two-phase cores. These were observed in the outer flow channel. They are (a) oil & gas/oil/water, (b) water & gas/oil/water, (c) oil & oil/oil/water, and (d) oil & water/oil/water. The scale bar is 100 μm.

We utilized diverse fluids to synthesis double emulsion with two-phase cores with different combination. Fig. 4 shows the typical types of double emulsion with two-phase cores in our experiments.

Structure evolution in reaching the different equilibrium morphologies

From the above results, we prepared four different double emulsions systems with inner two-phase cores. Then, we observed the structure evolution of the double emulsions. The stable morphology picture of every system is taken in a glass culture dish filled with outer phase. We took a lot of photos to show the detailed evolution progress of three different structures, as shown in Fig. 5. Fig. 5a shows the evolution of oil & oil/oil/water double emulsion, in which tetradecane and silicon oil (100 cp without surfactant) formed two inner droplets. They coalesce rapidly and form a Janus structure inside the middle phase TPGDA microcapsule. What is more interesting, the tetradecane first formed a Janus structure with TPGDA before it

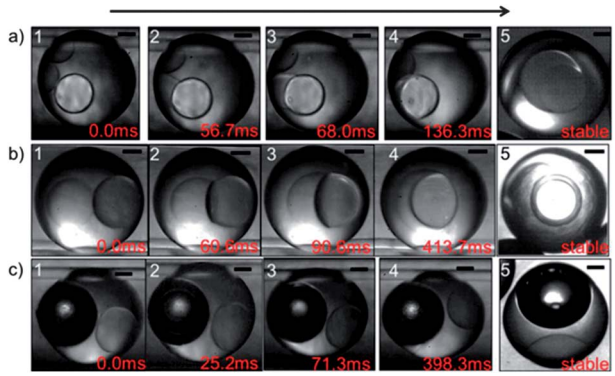

Fig. 5 The evolution of two inner droplets to their equilibrium morphologies in detail. Photo series 1–4 were observed in the outer flow channel, while photo series 5 were observed in the dish filled with outer phase. (a) Tetradecane and silicon oil (100 cp) evolved from two separate droplets to an Janus structure inside the TPGDA droplet in 200 ms around. The smaller inner droplet is tetradecane while the bigger one is silicon oil (100 cp). (b) Mineral oil and silicon oil (100 cp) evolved from two separate droplets to a triple emulsion in about 600 ms. Mineral oil was engulfed by silicon oil in the equilibrium morphology. (c) Tetradecane and air evolved from two separate droplets to a Janus structure and an engulfed structure separately in about 400 ms. The middle phase and the outer phase are TPGDA and deionized water with 2.0 wt% SDS and 1 wt% PVA. The evolution process can be seen in ESI as Movie S3–S5.† The scale bar is 100 μm.

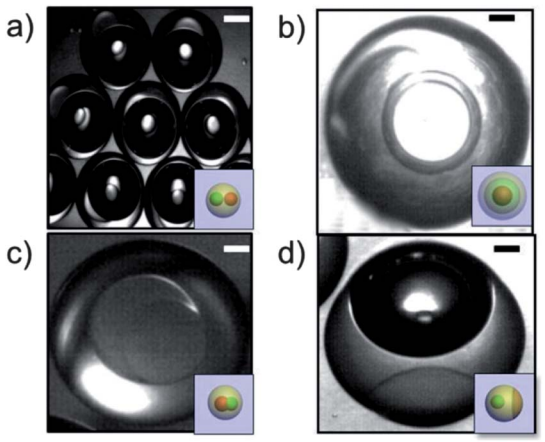

Fig. 6 Microphotographs of four typical equilibrium morphologies of double emulsions with two-phase cores. (a) Separately engulfing structure, namely inner droplets remained apart inside the middle phase droplet. The black droplet is gas and the other droplet is water. The gas floating above water because of density difference when we take this picture. (b) Triple emulsion structure. (c) Inner-Janus structure, namely inner droplets coalesced and then formed a Janus structure inside the middle phase droplet. (d) Janus-engulfing structure, which means one droplet formed a Janus with the middle phase droplet while the other one was surrounded inside it. The systems are (a) water + 1% (w/w) PVA + 2% (w/w) SDS & gas/silicon oil (50 cp) + 10% (w/w) Dow Corning 749/water + 1% (w/w) PVA + 2% (w/w) SDS; (b) silicon oil (50 cp) & mineral oil/TPGDA/water + 1% (w/w) PVA + 2% (w/w) SDS; (c) tetradecane & silicon oil (100 cp)/TPGDA/water + 1% (w/w) PVA + 2% (w/w) SDS; (d) tetradecane & air/TPGDA/water + 1% (w/w) PVA + 2% (w/w) SDS. The scale bar depicts 100 μm.

connected with the silicon oil, then it coalesced with silicon oil droplet to form a Janus structure within the TPGDA capsule. When the emulsion became stable, the Janus structure remained in the center of TPGDA droplet as shown in Fig. 5a-5. The process was then repeated, replacing the tetradecane with mineral oil, and this change of a single inner phase greatly affected the evolutionary process and equilibrium morphology as shown in Fig. 5b. The two inner droplets remained inside the whole time and coalesced step by step until the mineral oil was totally surrounded by the silicon oil, forming a triple emulsions (Fig. 5b-5). This also offers us a novel and simple approach for forming triple emulsions. Fig. 5c shows another morphology in which two inner droplets separated in a steady state when we replaced the silicon oil with air thus making the inner phases a combination of oil and gas. The two inner droplets remained apart the whole time with the microbubble engulfed by the TPGDA microcapsule while the tetradecane formed a Janus structure with the TPGDA (Fig. 5c-5). From the above results, different equilibrium structures can be formed when different combinations of inner phases were used in producing double emulsion with two-phase cores.

By changing phases, species and sequence of flows, we finally got four combinations of inner phases. They are combinations of aqueous phase and oil phase, aqueous phase and gas phase, oil phase and gas phase, and two immiscible oil phases. Furthermore, we obtained four typical equilibrium morphologies of these four-phase systems. They are separately engulfing structure (Fig. 6a), triple emulsion structure (Fig. 6b), inner-Janus structure (Fig. 6c) and Janus-engulfing structure (Fig. 6d). The separately engulfing structure is formed when two inner droplets separate from each other completely, and they tend to remain apart in the equilibrium state. The triple emulsion structure means that the inner two droplets get coalescence when they come in contact and then one phase surrounds the other phase to finally form a triple emulsion. The inner-Janus structure is a novel structure with two inner droplets form a Janus structure within the middle phase droplet. The Janus-engulfing structure is formed when the two inner droplets keep apart with each other and one forms a Janus structure with the middle phase droplet while the other one is surrounded inside it.

Physical mechanism in the equilibrium morphology of double emulsion with two-phase cores

The interfacial tensions of the four-phase systems were measured using the pendant drop method to determine the relationship between interfacial tension and equilibrium morphology. In order to use the spreading coefficient in our analysis, we divided each four-phase system into three three-phase groups: the two inner phases and the middle phase, one inner phase, the middle phase and the outer phase, and finally, the other inner phase, the middle phase and the outer phase. We measured the interfacial tension δ_{ij} between fluid i and j and calculated the spreading coefficient $S_i = \delta_{jk} - (\delta_{ij} + \delta_{ik})$ to predict the equilibrium morphology of the three-phase systems by using the prediction formula developed by Torza *et al.*[23] and Pannacci *et al.*,[21] where: (1) $S_1 < 0$, $S_2 > 0$, $S_3 < 0$, results in the formation of non-engulfing structures; (2) $S_1 < 0$, $S_2 < 0$, $S_3 > 0$,

Table 1 The spreading coefficient and equilibrium morphology of different systems[a]

	Phase 1	Phase 2	Phase 3	S_1	S_2	S_3	Morphology
1	Air	TPGDA	Tetradecane	−51.4	1.1	−2.6	Non-engulfing
2	Water[a]	Silicon oil[a]	Air	−48.7	20.9	−21.4	Non-engulfing
3	Silicon oil[b]	TPGDA	Mineral oil	−11.9	−9.4	8.6	Completely engulfing
4	Air	Water[a]	TPGDA	−54.8	−15.3	4.5	Completely engulfing
5	Silicon oil[a]	Water[a]	TPGDA	−9.7	−18.1	7.3	Completely engulfing
6	Air	TPGDA	Silicon oil[b]	−28.3	−22.0	0.7	Completely engulfing
7	tetradecane	Water[a]	TPGDA	−1.3	−10.5	−0.3	Partial engulfing
8	Silicon oil[a]	Water[a]	HDDA	−5.4	−22.4	−0.6	Partial engulfing
9	Water[b]	Octanol	Air	−1.8	−5.6	−52.6	Partial engulfing

[a] Water[a] here means water + 1% PVA + 2% SDS. Water[b] means water + 0.5% Tween80. Silicon oil[a] refers to silicon oil (50 cp) with Dow corning 749 (10 wt%). Silicon oil[b] refers to silicon oil (100 cp) without surfactant. In Row 3, the mineral oil was engulfed by silicon oil[b]. In Row 4, air was engulfed in TPGDA. In Row 5, TPGDA is engulfed in Silicon oil[a]. In Row 6, air is engulfed in silicon oil[b].

results in the formation of completely engulfing structures, and (3) $S_1 < 0$, $S_2 < 0$, $S_3 < 0$, results in the formation of partial engulfing structures. Table 1 and Fig. 7 show the relationship between morphology and spreading coefficient for all of the three-phase groups involved in our experiments. Specific interfacial tensions are listed in the ESI (see Table S1†).

The above analysis was used to determine the mechanism by which these double emulsions with two cores reached their equilibrium morphology. Firstly, the spreading coefficients of the three-phase group consisting of two inner phases and a middle phase were used to predict the equilibrium morphology. If this three-phase group were predicted to form a non-engulfing structure, when a fourth phase was added, the two inner droplets would remain separated within the middle phase droplet. However, when the spreading coefficients of the three-phase group predicted the formation of a complete-engulfing structure or a Janus structure, the two inner droplets coalesced within the middle phase droplet. Based on these observations, we then classified each of the four-phase systems as either separated inner droplet systems or coalescing inner droplet systems. For the first case, in which the two inner droplets remained separated, we analyzed the spreading coefficients of the other two three-phase groups (consisting of one of the inner phases, the middle phase and the outer phase) to predict their equilibrium morphology. By combining the predicted morphologies of these groups, we obtained the equilibrium morphology of double emulsions with two cores. For the second case in which the two inner droplets coalesced, we obtained the equilibrium morphology of the double emulsions with two cores directly without taking the other two three-phase groups into account.

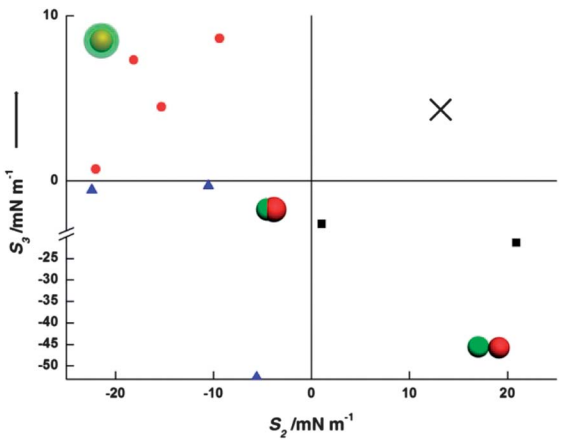

Fig. 7 The relationship between morphology and spreading coefficient for different three-phase systems in our experiments. Black squares represent non-engulfing, blue triangles partial engulfing and red circles completely engulfing. Cross represents this area is a physically inaccessible region.[21]

For example, to predict the equilibrium morphology of the tetradecane & air/TPGDA/water + 1% PVA + 2% SDS system, we first analyzed the spreading coefficient of the three-phase system consisting of tetradecane, air and TPGDA (data is shown in Row 1 of Table 1), predicting the formation of a non-engulfing structure as the equilibrium morphology of the three-phase group. Because the inner droplets remained separated throughout the process we then continued to examine the predicted equilibrium morphology of the other two three-phase groups. Then we analyzed the other three-phase systems which were air/TPGDA/water + 1% PVA + 2% SDS system and tetradecane/TPGDA/water + 1% PVA + 2% SDS system. The data of the two three-phase system were shown in Row 4 and 7 of Table 1, predicting that the equilibrium morphologies were complete-engulfing structure and partial engulfing structure, respectively. By combining the equilibrium morphologies, we predicted that the four-phase system formed a Janus-engulfing structure, just the same as the morphology they evolved into in our experimental condition, as shown in Fig. 6d. When we analyzed another four-phase system, which was silicon oil (50 cp) & mineral oil/TPGDA/water + 1% (w/w) PVA + 2% (w/w) SDS system, the similar analytical sequence was followed. First, we analyze the three-phase system consisting of silicon oil, mineral oil and TPGDA. The data was shown in Row 3 of Table 1, predicting that the equilibrium morphology was completely engulfing structure. And the inner droplets coalescence when they connect each other as we hypothesized in the above, which indicated that the four-phase system belonged to the second type. Then we could predict the equilibrium morphology of the four-phase system by surrounding the three-phase system with the fourth phase, thus a triple emulsion structure were obtained directly without

considering the other two three-phase systems. The prediction is also consistent with the experimental result, as shown in Fig. 6b. The other two typical structures shown in Fig. 6a and c could also be predicted in the same method.

Fig. 8 shows the visual description of the mechanism in predicting equilibrium morphology of double emulsions with two-phase cores in our experiments. In this figure, green and red phases represent two inner phases, yellow phase represents the middle phase and blue phase represents the outer phase. The three three-phase systems are: red phase/green phase/yellow phase, red phase/yellow phase/blue phase and green phase/yellow phase/blue phase. When the three-phase systems are considered, their equilibrium morphologies are determined by the theory of spreading coefficient.[23] The equilibrium morphology of red phase/green phase/yellow phase is used to identify the inner two droplets structure. If the morphology is non-engulfing structure, the inner two droplets remain separated; if the morphology is completely engulfing structure or partial engulfing structure, the inner droplets coalescence inside the middle phase droplet. When the fourth phase is taken into account, the morphology of double emulsions is decided in different method depending on which type the system belonged to. For the separated inner droplet systems in which the two inner droplets keep apart with each other, we have to take the other two three-phase systems as red phase/yellow phase/blue phase and green phase/yellow phase/blue phase into account by combining their morphologies. The four-phase system shown in Fig. 8a, whose two inner droplets keep apart and two three-phase systems both form completely engulfing structures, thus the equilibrium morphology of which is a separately engulfed structure; the four-phase system shown in Fig. 8b, whose two inner droplets remain separated and one three-phase system forms completely engulfing structure while the other one forms a Janus structure, thus the equilibrium morphology of which is a Janus-engulfing structure. These are the typical examples of the first type systems. For coalescing inner droplet systems, in which the two inner droplets get coalescence, we can obtain the equilibrium morphologies of four-phase systems more easily. The four-phase system shown in Fig. 8c, whose two inner droplets coalescence and form Janus structure, thus the equilibrium morphology of which is a inner-Janus structure and the four-phase system shown in Fig. 8d, whose two inner droplets coalescence and form a completely engulfed structure, thus the equilibrium morphology of which is a triple emulsion structure, are the typical examples of the second type systems.

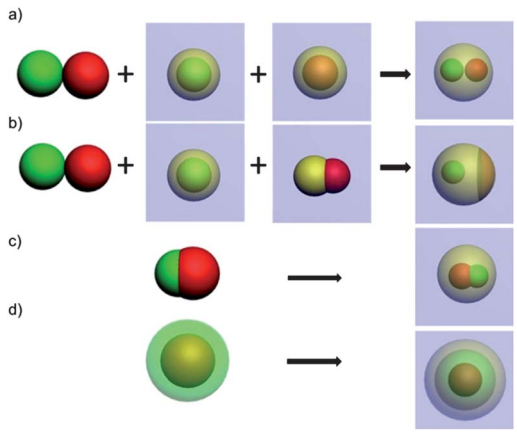

Fig. 8 The description of the evolution of double emulsions with two-phase cores. For the first type, in which the two inner droplets keep apart with each other, we have to take the both three-phase systems as one inner phase/middle phase/outer phase into account by combining their morphologies. (a) Two three-phase systems form completely engulfing structures, thus the equilibrium morphology is a separately engulfing structure. (b) One three-phase system forms a completely engulfing structure, while the other one forms a Janus structure, thus the equilibrium morphology is a Janus-engulfing structure. For the second type, in which the two inner droplets get coalescence, we can obtain the four-phase systems directly. For instance, (c) the two inner droplets form a Janus structure, thus the equilibrium morphology the four-phase systems is a inner-Janus structure. (d) The two inner droplets form a completely engulfing structure, thus the equilibrium morphology of the four-phase systems is a triple emulsion structure.

Microparticles with novel morphology

When abundant equilibrium morphologies are obtained, we could produce particles with new structures for wider

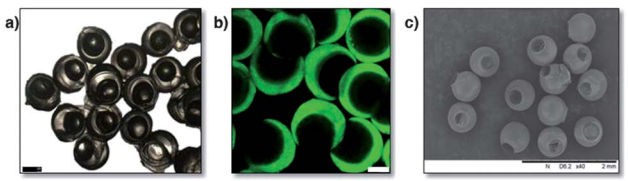

Fig. 9 Pictures of particles with Janus-engulfing structure. The system is silicon oil and gas/HDDA/water. (a) micrographic graph of particles, bubble are black and engulfed in silicon Janus semi-sphere. (b) Laser confocal fluorescence images. After UV light irradiation, HDDA in which quantum dot (CdSe/ZnS 565 nm) were dissolved was cured to particles and formed a crescent structure. (c) SEM pictures of Janus-engulfing structure. They formed hollow Janus particles. The scale bar in (a) and (b) depict 200 μm.

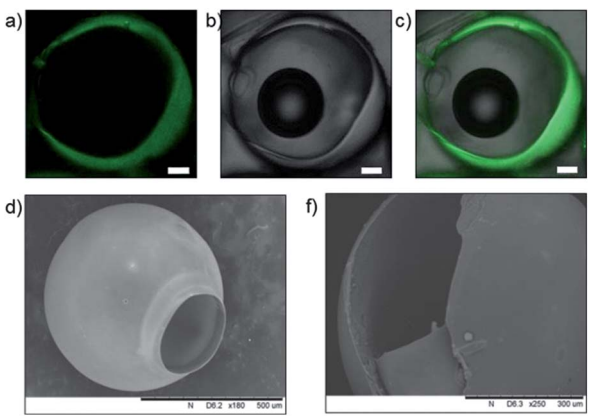

Fig. 10 The structures of a single microparticle. (a–c) are laser confocal fluorescence image, microscopic images, and their combination image of the same microparticle, respectively. (d) and (f) are SEM pictures, (d) shows the integrated structure of a Janus microparticle. (f) shows the inner hollow part when we crack the particle with a tweezer. The scale bar in (a–c) depict 100 μm.

application. For example, Janus-engulfing structure, with its Janus structure, can form an asymmetrical sphere with a thinner shell in one direction while thicker in another position, thus offers a perfect condition for the drug dissolved in the engulfing inner droplet to release from the thinner direction to obtain oriented release purpose. Particle with Janus-engulfing structure has been formed by utilizing a photo curable monomer as middle fluid. The system is gas & silicon oil/HDDA with 2% photo initiator/water + 1% PVA + 2% SDS. Silicon oil, which forms a Janus structure with HDDA, and gas, which is engulfed in silicon oil, were both used as inner fluids. For the equilibrium morphology, we could obtain these particles with narrow size distribution and similar structures, just shown in Fig. 9. Fig. 10 shows us more details about the micro particle. So this gives us a simple and novel approach to prepare microparticles with complex and well-controlled structures by utilizing different equilibrium morphologies made of double emulsions with two-phase cores.

Conclusions

In conclusion, we firstly prepare double emulsion with two-phase inner cores for different phases by using a simple one-step microfluidic approach. Inner two droplets combinations include oil and water, oil A and oil B, oil and gas, water and gas. Based on it, the structure evolution processes of the double emulsions for different systems were systemically studied. And we successfully obtained different multiple emulsions with four typical inner structures, as separately engulfing structure, triple emulsion structure, Janus-engulfing structure, and inner-Janus structure. Moreover, interfacial tensions between each immiscible phase are measured and analyzed to explain the relationship between the equilibrium morphology and the interfacial tensions of these four-phase systems. Finally, we use the theory of spreading coefficient to predict the equilibrium morphology of double emulsions with two-phase cores by classifying the four-phase system to three triple fluid systems.

The different equilibrium structures of these four-phase emulsion systems after the evolution of double emulsions with two-phase cores allow the synthesis of microparticles with new morphologies and encapsulation of multiple active substances, which is widely used in food science, cosmetics, pharmaceutics, and biomedical areas. In the future work, we will use these novel and complex four-phase emulsion systems to prepare microparticles with new morphologies or multi-functional microcapsules. For example, we can use the separately engulfing structure to prepare microcapsules for co-encapsulation and controlled release of water-soluble and oil-soluble active substances in the cores.

Acknowledgements

The authors gratefully acknowledge the supports of the National Natural Science Foundation of China (21322604, 21136006, 21036002), National Basic Research Program of China (2012CBA01203) and A Foundation for the Author of National Excellent Doctoral Dissertation of PR China (FANEDD 201053).

Notes and references

1 C. Laugel, A. Baillet, M. P. Y. Piemi, J. P. Marty and D. Ferrier, *Int. J. Pharm.*, 1998, **160**(1), 109–117.
2 L. Myung Han, K. C. Hribar, T. Brugarolas, N. P. Kamat, J. A. Burdick and L. Daeyeon, *Adv. Funct. Mater.*, 2012, **22**(1), 131–138.
3 B. Raghuraman, N. Tirmizi and J. Wiencek, *Environ. Sci. Technol.*, 1994, **28**(6), 1090–1098.
4 K. J. Lissant, B. W. Peace, S. H. Wu and K. G. Mayhan, *J. Colloid Interface Sci.*, 1974, **47**(2), 416–423.
5 M. Gallarate, M. E. Carlotti, M. Trotta and S. Bovo, *Int. J. Pharm.*, 1999, **188**(2), 233–241.
6 J. H. Xu, H. Zhao, W. J. Lan and G. S. Luo, *Adv. Healthcare Mater.*, 2012, **1**(1), 106–111.
7 J. Bibette, F. Leal-Calderon, V. Schmitt and P. Poulin, *Emulsion Science: Basic Principles - an Overview*, Springer, 2002.
8 S. Matsumoto, Y. Kita and D. Yonezawa, *J. Colloid Interface Sci.*, 1976, **57**(2), 353–361.
9 L. Y. Chu, A. S. Utada, R. K. Shah, J. W. Kim and D. A. Weitz, *Angew. Chem., Int. Ed.*, 2007, **46**(47), 8970–8974.
10 H. C. Shum, Y.-j. Zhao, S.-H. Kim and D. A. Weitz, *Angew. Chem., Int. Ed.*, 2011, **50**(7), 1648–1651.
11 H. Y. Chen, Y. Zhao, Y. L. Song and L. Jiang, *J. Am. Chem. Soc.*, 2008, **130**(25), 7800–7801.
12 W. Wang, R. Xie, X. J. Ju, T. Luo, L. Liu, D. A. Weitz, L. Y. Chu and L. Y. Chu, *Lab Chip*, 2011, **11**(9), 1587–1592.
13 L. L. A. Adams, T. E. Kodger, S. H. Kim, H. C. Shum, T. Franke and D. A. Weitz, *Soft Matter*, 2012, **8**(48), 12132–12132.
14 S. K. Lee, X. Y. Liu, V. S. Cabeza and K. F. Jensen, *Lab Chip*, 2012, **12**(20), 4080–4084.
15 M. Shaohua, J. Thiele, L. Xin, B. Yunpeng, C. Abell and W. Huck, *Small*, 2012, **8**(15), 2356–2360.
16 T. S. Shim, S. H. Kim, J. Y. Sim, J. M. Lim and S. M. Yang, *Adv. Mater.*, 2010, **22**(40), 4494–4498.
17 W. Wang, C. Yao, M. J. Zhang, X. J. Ju, R. Xie and L. Y. Chu, *J. Phys. D: Appl. Phys.*, 2013, **46**(11), 114007–114014.
18 M. Seo, C. Paquet, Z. H. Nie, S. Q. Xu and E. Kumacheva, *Soft Matter*, 2007, **3**(8), 986–992.
19 W. J. Lan, S. W. Li, J. H. Xu and G. S. Luo, *Langmuir*, 2011, **27**(21), 13242–13247.
20 Z. H. Nie, S. Q. Xu, M. Seo, P. C. Lewis and E. Kumacheva, *J. Am. Chem. Soc.*, 2005, **127**(22), 8058–8063.
21 N. Pannacci, H. Bruus, D. Bartolo, I. Etchart, T. Lockhart, Y. Hennequin, H. Willaime and P. Tabeling, *Phys. Rev. Lett.*, 2008, **101**(16), 164502–164505.
22 S. Torza and S. G. Mason, *Science*, 1969, **163**(3869), 813–814.
23 S. Torza and S. G. Mason, *J. Colloid Interface Sci.*, 1970, **33**(1), 67–83.

